# Application of Energy-Dispersive X-ray Elemental Mapping To Probe the Homogeneity of Sol–Gel Derived $YBa_2Cu_3O_{7-\delta}$ and Related Phases

Carol S. Houk, Gary A. Burgoine, and Catherine J. Page*

*Department of Chemistry, University of Oregon, Eugene, Oregon 97403*

*Received August 2, 1994. Revised Manuscript Received January 18, 1995*[⊗]

Energy-dispersive X-ray (EDX) elemental mapping has been used to assess the homogeneity of solid state products of a sol–gel synthetic route developed for the synthesis of $YBa_2Cu_3O_{7-\delta}$. Transmission electron microscopy (TEM), X-ray diffraction (XRD), FTIR, iodometric titration, elemental analysis, and magnetic susceptibility have been used to probe the homogeneity and phase composition at various stages of the sol–gel process. The starting solutions contain stoichiometric amounts of the metal 2-(2-methoxyethoxy)ethoxide components in 2-(2-methoxyethoxy)ethanol and appear to be homogeneous by TEM with particle sizes less than 2 nm. While XRD suggests that products of sol–gel synthesis and conventional solid-state synthesis fired to 950 °C are single-phase orthorhombic $YBa_2Cu_3O_{7-\delta}$, magnetic susceptibility measurements indicate that both samples have two superconducting phases, and the EDX elemental maps of each show considerable micrometer-scale inhomogeneities. Sol–gel derived products processed at 700 °C for 48 h appear to be tetragonal by XRD; additional data suggest that the dominant phase is the tetragonal oxycarbonate phase ($YBa_2Cu_3(CO_3)_{0.2}O_{6.7}$). Elemental maps show a more homogeneous distribution of the component metals in this material, but some zoning is seen in the irregularly shaped particles, suggesting a nonequilibrium product. When the gel is fired at 700 °C for 2 weeks, an orthorhombic $YBa_2Cu_3O_{7-\delta}$ XRD pattern is observed, and magnetic susceptibility shows a single superconducting phase, with an 88 K transition temperature. Elemental maps show the product to be highly homogeneous in elemental distribution within particles. These results indicate that this alkoxide sol–gel route can yield high-quality $YBa_2Cu_3O_{7-\delta}$ at 700 °C but that kinetic effects are important in this low-temperature synthetic route.

## Introduction

Alkoxide sol–gel synthesis involves the hydrolytic condensation of a metal alkoxide solution to produce a gel, which can be fired to form glasses or crystalline metal oxides. Ideally, when applied to the synthesis of complex oxides (those containing more than one type of metal cation), the metal alkoxide components of the starting solution are homogeneously mixed on the molecular level. Upon hydrolysis this molecular-scale homogeneity is maintained throughout the gelation process, and firing should result in products superior in quality to products of conventional solid-state synthesis.[1–4] Also, in principle the desired ceramic material should be obtainable at lower temperatures and/or in less time since diffusion barriers in the sol–gel process are significantly lower than those in the conventional solid state method. In reality, however, the alkoxide sol–gel synthesis of complex oxides is often plagued by the limited solubility of one or more of the component alkoxides, differences in hydrolysis rates of the individual components, and the formation of contaminants (such as carbonates), all of which can lead to micrometer-scale inhomogeneity via metal component separation during hydrolysis and gelation. Separation of component metals can also occur during the firing process due the formation of phases more stable than the target compound at low processing temperatures.[5]

The synthesis of $YBa_2Cu_3O_{7-\delta}$ by the alkoxide sol–gel method has been plagued by the insolubility of copper(II) alkoxides,[6–8] the relatively faster gelation rate of some yttrium alkoxides,[9] and the formation of $BaCO_3$.[10–13] In addition, several bimetallic compounds in the Y/Ba/Cu/O phase diagram are relatively more stable than the target compound at low firing temperatures.[5,14]

The problem of the general insolubility of copper(II) alkoxides has been circumvented in a variety of ways.

[⊗] Abstract published in *Advance ACS Abstracts,* March 1, 1995.

(1) Lee, G. R.; Crayston, J. A. *Adv. Mater.* **1993**, *5*, 434.
(2) Mehrotra, R. C. *J. Non-Cryst. Solids* **1988**, *100*, 1.
(3) Schmidt, H. *J. Non-Cryst. Solids* **1988**, *100*, 51.
(4) Reuter, H. *Adv. Mater.* **1991**, *3*, 258.
(5) Rupich, M. W.; Liu, Y. P.; Ibechem, J.; Hachey, J. P. *J. Mater. Res.* **1993**, *8*, 1487.
(6) Monde, T.; Kozuka, H.; Sakka, S. *Chem. Lett.* **1988**, 287.
(7) Ravindranathan, P.; Komarneni, S.; Bhalla, A.; Roy, R.; Cross, L. E. *J. Mater. Res.* **1988**, *3*, 810.
(8) Kramer, S. A.; Kordas, G.; McMillan, J.; Hilton, G. C.; Van Harligen, J. D. *Appl. Phys. Lett.* **1988**, *253*, 156.
(9) Moore, G.; Kramer, S.; Kordas, G. *Mater. Lett.* **1989**, *7*, 415.
(10) Kordas, G.; Moore, G. A.; Jorgensen, J. D.; Rotella, F.; Hitterman, R. L.; Volin, K. J.; Faber, J. *J. Mater. Chem.* **1991**, *1*, 175.
(11) Katayama, S.; Sekine, M. *J. Mater. Res.* **1990**, *5*, 683.
(12) Horowitz, H. S.; McLain, S. J.; Sleight, A. W.; Druliner, J. D.; Gai, P. L.; VanKavelaar, M. J.; Wagner, J. L.; Biggs, B. D.; Poon, S. J. *Science* **1989**, *243*, 66.
(13) Hirano, S.; Hayashi, T.; Miura, M.; Tomonaga, H. *Bull. Chem. Soc. Jpn.* **1989**, *62*, 888.
(14) Garson, F. H.; I. D., R.; Ginley, D. S.; Halloran, J. W. *J. Mater. Res.* **1991**, *6*, 885.

0897-4756/95/2807-0649$09.00/0 © 1995 American Chemical Society

Modifiers such as carboxylic acids,[15] amines,[6,11] or acetylacetonate[16,17] can be used to form more soluble modified copper alkoxide complexes, or the solubility in nonpolar solvents can be increased by ether alcohol ligand exchange to form copper etheralkoxides.[9,10,12,13,18,19] In the former case, coordination of these additives to the metal centers disrupts the formation of a metal–oxygen network since they do not undergo hydrolysis or condensation reactions. Furthermore, because the modifying ligands do not hydrolyze, their use will in principle yield intermediates with a higher carbon content. For these reasons the latter approach is preferred, since the ether alkoxide ligands will undergo hydrolysis; however, the use of a nonpolar solvent is not optimal, particularly if it is immiscible with water.

We have made use of a complexation reaction between copper and barium diol or ether alcohol salts which produces a bimetallic barium–copper complex which is soluble in the parent diol or ether alcohol. For diol salts and 2-methoxyethanol salts, soluble complexes with a 1:1 Ba:Cu ratio have been observed for a number of systems.[17,18,20,21] Using copper and barium 2-(2-methoxyethoxy)ethoxides in 2-(2-methoxyethoxy)ethanol, we have taken advantage of this type of complexation reaction to obtain solutions containing a 2:3 ratio of barium to copper.[20,22,23] While we have not been able to isolate crystals of the bimetallic ether alkoxide complex(es) for structure determination, we believe the interaction between the barium and copper ether alkoxide centers is similar to that of a structurally characterized barium–copper ethylene glycol complex.[20] Addition of yttrium isopropoxide yields a starting solution containing stoichiometric amounts of each metal component for the synthesis of $YBa_2Cu_3O_{7-\delta}$. Although we have no direct evidence that the yttrium component is incorporated into a bi- or trimetallic species with barium or the barium–copper complex, respectively, we have observed that the yttrium component is more soluble in the presence of the barium–copper complex.

The rate of gelation upon the addition of $H_2O$ is dependent not only on the particular metal components involved but also on the hydrolysis ratio, pH, alkoxide concentration of the starting solution, exposed surface area, atmospheric humidity, and temperature.[1–4] In the Y/Ba/Cu/O system these parameters can also affect the formation of $BaCO_3$ during gelation, and studies are underway to determine the specific conditions which favor $BaCO_3$ formation. Except for changing the identity of the metal components, we have studied each of the above parameters to develop a set of conditions which generally gives carbonate-free gels in approximately 2 weeks.

In the conventional solid-state synthesis of $YBa_2Cu_3O_{7-\delta}$, a stoichiometric mixture of metal oxides and/or carbonates is fired to 925–950 °C for 24–48 h to produce the tetragonal nonsuperconducting $YBa_2Cu_3O_{7-\delta}$ phase ($0.5 \leq \delta \leq 1.0$). Slow cooling and subsequent annealing in oxygen between 450 and 650 °C for less than 24 h[24] gives the orthorhombic superconducting $YBa_2Cu_3O_{7-\delta}$ phase ($0.0 \leq \delta \leq 0.5$). The orthorhombic phase is more stable than the tetragonal phase at temperatures lower than 590 °C (at ambient pressure) but the high initial firing temperature (925–950 °C) is required to overcome solid-state diffusion barriers.[25,26]

In principle, sol–gel synthesis should provide reactants with an intimate mixture of metal components so that high temperatures are not necessary for diffusion to mix them. In the more than 100 literature reports of sol–gel derived $YBa_2Cu_3O_{7-\delta}$ pyrolysis temperatures ranging from 650 to 950 °C have been used with varying success. In general, while the superconducting orthorhombic phase should be stable at temperatures lower than 590 °C, no direct sol–gel synthesis of the orthorhombic phase has been reported at such low temperatures. In fact, most low-temperature (650–850 °C) synthetic routes which involve carbon-containing precursors result in a tetragonal oxycarbonate phase, $YBa_2Cu_3(CO_3)_xO_{7-\delta}$.[25,27–29] While sol–gel products fired to ~950 °C do generally give orthorhombic superconducting product, the potential low-temperature processing advantage is not achieved in this case, and there is no direct evidence that sol–gel products are of higher quality than conventionally prepared materials.

We report here the sol–gel synthesis of orthorhombic $YBa_2Cu_3O_{7-\delta}$ prepared at temperatures as low as 700 °C using homogeneous starting solutions of yttrium, barium, and copper 2-(2-methoxyethoxy)ethoxides in 2-(2-methoxyethoxy)ethanol. We also compare sol–gel and conventionally prepared products fired to 950 °C. Characterization of products is accomplished through X-ray diffraction, elemental analysis, IR spectroscopy, microscopy (SEM and TEM), iodometric titrations, magnetic susceptibility, and energy-dispersive X-ray (EDX) elemental mapping.

The previous use of EDX elemental mapping for assessing homogeneity of $YBa_2Cu_3O_{7-\delta}$ has been limited.[30–39] Several of these previous studies used

(15) Zheng, H.; Mackenzie, J. D. *Mater. Lett.* **1988**, *7*, 182.
(16) Catania, P.; Hovnanian, N.; Cot, L.; Pham Thi, M.; Kormann, R.; Ganne, J. P. *Mater. Res. Bull.* **1990**, *25*, 631.
(17) Sauer, N. N.; Garcia, E.; Salazar, K. V.; Ryan, R. R.; Martin, J. A. *J. Am. Chem. Soc.* **1990**, *112*, 1524.
(18) Goel, S. C.; Kramer, K. S.; Gibbons, P. C.; Buhro, W. E. *Inorg. Chem.* **1989**, *28*, 3619.
(19) Kordas, G. *J. Non-Cryst. Solids* **1990**, *121*, 436.
(20) Love, C. P.; Torardi, C. C.; Page, C. J. *Inorg. Chem.* **1991**, *31*, 1784.
(21) Purdy, A. P.; George, C. F. *Inorg. Chem.* **1991**, *30*, 1969.
(22) Page, C. J.; Houk, C. S.; Burgoine, G. A. *Mater. Res. Soc. Symp. Proc. (Better Ceramics Through Chemistry V)* **1992**, *271*, 155.
(23) Houk, C. S.; Burgoine, G. A.; Page, C. J. *Mater. Res. Soc. Symp. Proc. (Better Ceramics Through Chemistry VI)* **1994**, *346*, 29.
(24) Cava, R. J.; Batlogg, B.; van Dover, R. B.; Murphy, D. W.; Sunshine, S.; Siegrist, T.; Remeika, J. P.; Rietman, E. A.; Zahurak, S.; Espinosa, G. P. *Phys. Rev. Lett.* **1987**, *58*, 1676.
(25) Karen, P.; Braaten, O.; Kjekshus, A. *Acta Chem. Scand.* **1992**, *52*, 805.
(26) Wang, H.; Li, D. X.; Thomson, W. J. *J. Am. Ceram. Soc.* **1988**, *71*, C-1988.
(27) Boullay, P.; Domenges, B.; Hervieu, M.; Raveau, B. *Chem. Mater.* **1993**, *5*, 1683.
(28) Gotor, F. J.; Odier, P.; Gervais, M.; Choisnet, J.; Monod, P. *Physica C* **1993**, *218*, 429.
(29) Karen, P.; Kjekshus, A. *J. Solid State Chem.* **1991**, *94*, 298.
(30) Goldstein, E. A. In *Scanning Electron Microscopy and X-Ray Microanalysis*; Plenum Press: New York, 1992; p 525.
(31) Marinenko, R. B. *Microbeam Anal.* **1991**, 333.
(32) Newbury, D. E.; Marinenko, R. B.; Myklebust, R. L.; Bright, D. S. In *Electron Probe Quantitation*; Heinrich, K. F. J., Newbury, D. E., Ed.; Plenum Press: New York, 1991; pp 335–369.
(33) Madhavrao, L.; Rajagopalan, R. *J. Mater. Science* **1990**, *25*, 2349.
(34) Newbury, D. E.; Fiori, C. E.; Marinenko, R. B.; Myklebust, R. L.; Swyt, C. R.; Bright, D. S. *Anal. Chem.* **1990**, *62*, 1159.
(35) Verkouteren, J. R. *Mater. Lett.* **1989**, *8*, 59.
(36) Blendell, J. E.; Handwerker, C. A.; Vaudin, M. D.; Fuller, J., E. R. *J. Cryst. Growth* **1988**, *89*, 93.
(37) Marinenko, R. B.; Newbury, D. E.; Bright, D. S.; Myklebust, R. L.; Blendell, J. E. *Microbeam Anal.* **1988**, 37.
(38) Friel, J. J.; Juzwak, T. J.; Johnson, P. F. *Microbeam Anal.* **1988**, 41.

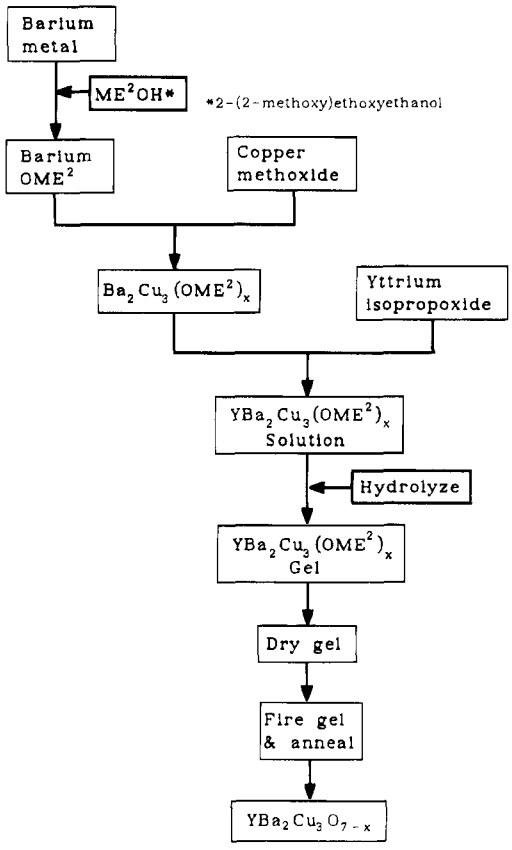


**Figure 1.** Flowchart of synthesis.

elemental mapping to determine the extent of interaction between the superconductor and substrates, firing vessels, or electrodes;[31,33,35] others have used EDX elemental mapping to study microstructure, grain boundaries and to discern the presence of liquid phases during firing of powder-processed materials.[36–39] Advances in technology in this field along with careful sample preparation and instrument setup allow for near-photographic quality images of material on the micrometer scale. We have found this technique to be a valuable tool for evaluating the homogeneity and particle size distributions of our products. To our knowledge, the study reported here represents the first use of EDX elemental mapping to evaluate sol–gel products and the first to compare sol–gel derived $YBa_2Cu_3O_{7-\delta}$ with that produced using a solid-state synthetic route.

## Experimental Section

All manipulations of reactants, solvents, and alkoxide solutions prior to hydrolysis were carried out under purified nitrogen atmosphere, using either Schlenk glassware and vacuum-line techniques or an inert-atmosphere drybox. Barium metal granules were used as purchased from Alfa. Copper methoxide was prepared from a reaction of anhydrous copper chloride and excess lithium methoxide,[20] and yttrium oxoisopropoxide was prepared from a reaction of yttrium chloride and potassium isopropoxide.[40] 2-(2-Methoxy)ethoxyethanol was dried over sodium and distilled under vacuum. Figure 1 is a flowchart of the process used in our synthesis. Barium metal is dissolved in dry 2-(2-methoxy)ethoxyethanol, and a stoichiometric amount of copper methoxide is added. Sonification for approximately half an hour results in a clear royal blue solution. A stoichiometric amount of yttrium isopropoxide is then added, and the solution is sonicated for approximately 15 min. Resulting solutions are on the order of 0.05 M in metals. Samples for TEM imaging were prepared by spraying the solution onto carbon-coated copper or nickel support grids in an inert-atmosphere drybox and allowing them to dry. Comparison samples were sprayed in air as were hydrolyzed samples. The micrographs were made using a Philips CM-12 TEM/STEM operated at 100 kV with a 70 $\mu$m aperture.

Hydrolysis is induced by the addition of a 30% $H_2O_2$ aqueous solution in a 5:1 ratio of $H_2O$ to metals. Use of the 30% $H_2O_2$ aqueous solution for hydrolysis rather than purified water lowered the pH slightly and gave clearer gels. Hydrolyzed solutions are poured into Petri dishes, loosely covered, and allowed to gel over the period of 1 week. Once the gel is "set" it is aged for an additional week to maximize condensation. The gel is separated from the mother liquor through centrifugation, and the concentrated gel is dried in a stream of flowing nitrogen.

For the solid-state synthesis mixtures of stoichiometric amounts of $Y_2O_3$, $BaCO_3$, and CuO powders were finely ground by mortar and pestle. The particle size of these powders was not determined. Dried gels, as well as solid-state mixtures, were fired in alumina boats under 90% nitrogen/10% oxygen flowing at 100 sccm with an attached $CO_2$ scrubber (indicating soda lime). The firing temperature was ramped 2 °C/min to the pyrolyis temperature, and after firing was cooled at 1 °C/min to the annealing temperature and/or room temperature. Specific firing times and temperatures for samples discussed in this paper are given in Table 1 of the next section. Dried gels and fired products were characterized by powder X-ray diffraction (XRD) using a Scintag XDS-2000 $\theta-\theta$ powder diffractometer. Lattice parameters were determined using the Scintag DMS2000 Peakfinder and Lattice Refinement programs. Diffraction peaks from the aluminum sample support were used as an "internal standard" to correct for alignment errors. Yttrium, barium, copper, and carbon elemental analyses were performed by E + R Microanalytical Laboratories, Inc. Iodometric titrations for the determination of oxygen content were modified from Vlaeminck et al.[22] using inert-atmosphere techniques.

Magnetic susceptibility was measured from 2 to 270 K at fields of 2 and 4 kG using a computer-interfaced Faraday balance.

Compositional maps of fired samples were obtained with a JEOL JSM 6300/LINK EDX SEM/EDX (Oxford Instruments) operated at 20 kV and 6.5–7.0 nA. Data collection "windows" were defined from the characteristic peaks for each of the elements to be mapped from a representative X-ray spectrum for a sample of the orthorhombic $YBa_2Cu_3O_{7-\delta}$. Data were collected over a dwell time of 5 ms/pixel and 10 scans (50 ms/pixel total). This process of multiple scans increases the signal-to-noise ratio. Because the signal-to-noise ratio was quite high and because we did not endeavor to obtain quantitative compositional data, subtraction of Bremsstrahlung background and extensive comparison with well-characterized standards was not done. The intensity of the characteristic X-rays were given a value from 0 to 255 for each pixel by the LINK software, thus producing a digital "gray scale" image. These digital images were processed using Adobe Photoshop. Bright areas indicate a high concentration of the element and dark areas indicate an absence of the element.

## Results and Discussion

Prior to hydrolysis, solutions contained stoichiometric amounts of the metal components and had an average particle size of less than 2 nm as observed by TEM (Figure 2a). The same solution sprayed in air is seen in Figure 2b, which shows the initial effects of hydrolysis and condensation reactions which appear to produce an open, lacy network. As these reactions continue, the

(39) Blendell, J. E.; Chiang, C. K.; Cranmer, D. C.; Freiman, S. W.; Fuller, J., E. R.; Drescher-Krasicka, E.; Johnson, W. L.; Ledbetter, H. M.; Bennett, L. H.; Swartzendruber, L. J.; Marinenko, R. B.; Myklebust, R. L.; Bright, D. S.; Newbury, D. E. *Adv. Ceram. Mater.* **1987**, *2*, 512.
(40) Page, C. J.; Sur, S. K.; Lonergan, M. C.; Parashar, G. K. *Magn. Reson. Chem.* **1991**, *29*, 1191.

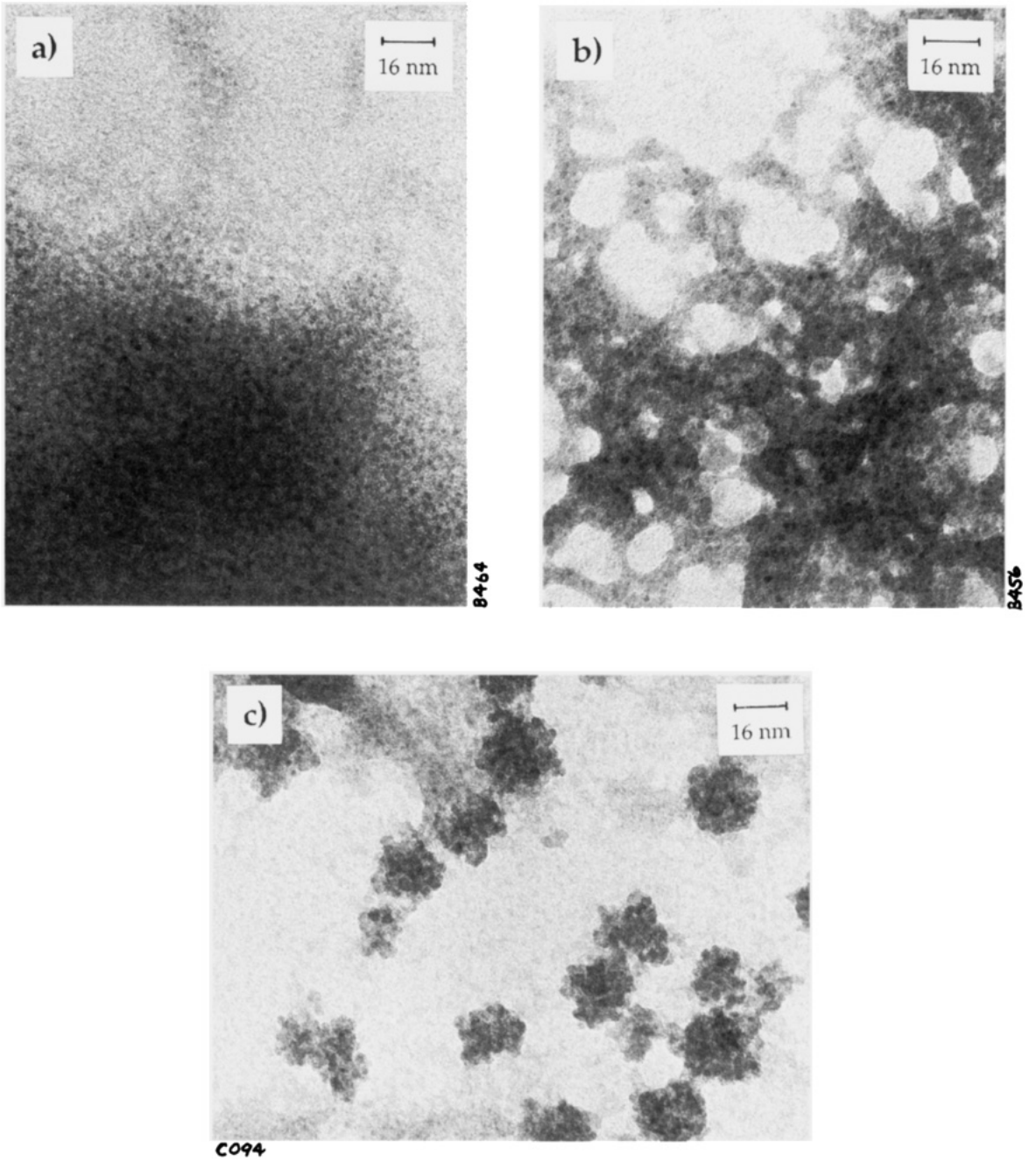


**Figure 2.** TEM micrographs of (a, top) fresh solution sprayed onto a carbon grid in $N_2$ atmosphere (edge of droplet imaged); (b, middle) fresh solution sprayed onto carbon grid in air; (c, bottom) hydrolyzed solution aged 6 days.

loose network condenses into the denser clusters seen in Figure 2c. Various studies by other groups have shown that these types of clusters sometimes aggregate into another more condensed network which can be modeled by fractals,[41-46] although we have not observed this phenomenon directly in this system. Attempts to assess the compositional homogeneity of solutions and wet gels using EDX lateral elemental mapping have so far been unsuccessful.

Powder X-ray diffraction patterns of dried gels are characteristic of amorphous materials and show no crystalline diffraction peaks. Thermal gravimetric analyses of air-dried gels show ~38% mass loss between 25 and 350 °C, and generally a very small residual mass loss between 400 and 1000 °C (~1% per 100 °C).[22] X-ray diffraction patterns of gels fired to 350 °C indicate that at this intermediate firing temperature (after most organic residues have been pyrolyzed) the product remains amorphous, with no observable crystalline impurity phases.

Table 1 gives the firing parameters for gels fired to higher temperatures which will be discussed in detail below. Sample A was conventionally synthesized from oxide and carbonate powders as noted in the experi-

(41) Ramsay, J. D. F. *Chem. Soc. Rev.* **1986**, *15*, 335.
(42) Chaumont, D.; Craievich, A.; Zarzycki, J. *J. Non-Cryst. Solids* **1992**, *147, 148*, 127.
(43) Kordas, G.; Moore, G. A.; Salamon, M. B.; Hayter, J. B. *J. Mater. Chem.* **1991**, *1*, 181.
(44) Kudoh, M.; Hu, X.; Ohno, K.; Kawazoe, Y. *J. Cryst. Growth* **1993**, *128*, 1162.
(45) Martin, J. E.; Wilcoxon, J. *Mater. Res. Soc. Symp. Proc. (Better Ceramics Through Chemistry IV)* **1990**, *180*, 199.
(46) Meakin, P. *Mater. Res. Soc. Symp. Proc. (Better Ceramics Through Chemistry IV)* **1990**, *180*, 141.
(47) Swinnea, J. S.; Steinfink, H. *J. Mater. Res.* **1987**, *2*, 424.

**Table 1. Firing Parameters and Results**

| sample | synthesis | temp (°C) | time | unit cell | lattice parameters (nm)[a] | | | $T_c$ (K) | % Meissner |
|---|---|---|---|---|---|---|---|---|---|
| | | | | | *a* | *b* | *c* | | |
| A | solid-state | 950 | 24 h | orthorhombic | 0.3827(2) | 0.3890(2) | 1.1681(4) | ~82, ~33 | 62 |
| B | sol–gel | 950 | 24 h | orthorhombic | 0.3831(4) | 0.3890(4) | 1.1666(9) | ~82, ~33 | 48 |
| C | sol–gel | 700 | 48 h | tetragonal | 0.3879(2) | | 1.1665(9) | | 0 |
| D | sol–gel | 700 | 2 weeks | orthorhombic | 0.3830(2) | 0.3890(2) | 1.1657(4) | 88 | 18 |
| $YBa_2Cu_3O_{6.8}$ | | ref 24 | | orthorhombic | 0.3822 | 0.3891 | 1.1681 | 91 | 76 |
| $YBa_2Cu_3O_{6.0}$ | | ref 47 | | tetragonal | 0.3863 | | 1.1830 | | |
| $YBa_2Cu_3(CO_3)_{0.2}O_{6.7}$ | | ref 29 | | tetragonal | 0.3874 | | 1.1612 | | |

[a] Determined by XRD. Estimated standard deviations in the last decimal place are given in parentheses.

**Table 2. Elemental Composition**

| element (mass %) | sample A | sample B | sample C | sample D | $YBa_2Cu_3O_{6.8}$[a] | $YBa_2Cu_3(CO_3)_{0.2}O_{6.7}$[a] |
|---|---|---|---|---|---|---|
| yttrium | 11.96 | 12.32 | 10.52 | 9.95 | 13.41 | 13.20 |
| barium | 40.24 | 40.91 | 37.01 | 40.85 | 41.43 | 40.79 |
| copper | 31.29 | 31.19 | 28.44 | 31.44 | 28.75 | 28.31 |
| carbon | 0.15 | 0.19 | 0.55 | 0.28 | | 0.36 |

[a] Calculated for formulas as shown.

mental section and was used as a reference for comparison with products made via the sol–gel technique. Sample B was prepared from a ground dried gel and was fired simultaneously with sample A in order to compare the two methods directly. These samples were fired only once and were not annealed.

Unit-cell symmetry and lattice parameters from XRD and superconducting properties determined by magnetic susceptibility studies are also summarized for samples A–D in Table 1. Unit-cell symmetry is assigned as orthorhombic or tetragonal on the basis of the splitting of certain diffraction peaks (e.g., the (103) and (013) lines, the (200) and (020) lines and the (123) and (213) lines, shown in Figure 3a). The tetragonal and orthorhomic $YBa_2Cu_3O_{7-\delta}$ phases have very similar lattice parameters (as given in Table 1). The splitting of certain peaks in the orthorhombic diffraction pattern is a consequence of oxygen ordering along the *b* axis, creating a small difference in the *a* and *b* parameters of this phase, which bracket the *a* value of the nonsuperconducting tetragonal phase. It is worth noting in this context that the lattice parameters of the tetragonal and orthorhombic $YBa_2Cu_3O_{7-\delta}$ phases given for comparison in Table 1 are from specific references. There are a range of values for these parameters in the literature, especially for the orthorhombic phase (values deviate from those given in Table 1 by 1 pm for *a* and *b*, and ~10 pm for *c*).[48] The range in reported values is sample dependent and is generally accepted to be a consequence of the variable oxygen content in this phase. It has been shown that the lattice parameters of this compound vary smoothly from the most orthorhombic ($YBa_2Cu_3O_7$; $\delta = 0$) to the tetragonal phase ($YBa_2Cu_3O_{6.5}$; $\delta = 0.5$) as a function of oxygen content.[48,49] Thus, varying degrees of orthorhombicity are possible between these extremes. The superconducting transition temperatures can also vary from ~93 K for $YBa_2Cu_3O_7$ to ~30 K for $YBa_2Cu_3O_{6.6}$.[49]

The results of yttrium, barium, copper, and carbon elemental analyses of samples A–D performed by E + R Microanalytical Laboratories, Inc. are given in Table 2. Data presented in Tables 1 and 2 will be discussed below in the context of other experimental data for each of the samples.

Figures 3 and 4 show the X-ray diffraction patterns, magnetic susceptibility data, and EDX lateral Y, Ba, and Cu elemental maps for samples A and B, respectively. The X-ray diffraction patterns for both samples (Figures 3a and 4a), and the refined lattice parameters (Table 1) are consistent with single-phase orthorhombic $YBa_2Cu_3O_{7-\delta}$. However, while samples A and B appear to be single phase by XRD, magnetic susceptibility data (Figures 3b and 4b) indicate the presence of two superconducting phases in both samples: one with a $T_c$ onset at ~82 K; the other with a $T_c$ onset at ~33 K. The phase with the higher $T_c$ is presumably orthorhombic $YBa_2Cu_3O_{7-\delta}$. The phase with a lower $T_c$ may be a more oxygen-deficient $YBa_2Cu_3O_{7-\delta}$ for which $\delta \sim 0.4$.[49] Formation of two distinct $YBa_2Cu_3O_{7-\delta}$ phases with different oxygen contents is possible in this case because the samples were not annealed under oxygen. The slow cooling from 950 °C in a nitrogen/oxygen mixture may have allowed for different degrees of oxygenation within the samples. This explanation could possibly account for the observation of two phases of similar oxygen content in both sample A (solid state synthesis) and sample B (sol–gel synthesis) since they were fired simultaneously. Alternatively, the lower $T_c$ phase could be $Y_2Ba_4Cu_7O_{14+x}$, for which a sample-dependent $T_c$ of ~40 K has been reported.[50] However, this latter possibility is unlikely since this phase is usually prepared at high oxygen pressures and because this phase is not observed in the diffraction pattern.

The field dependence of the susceptibilities indicate that the lower $T_c$ phase consists of smaller crystallites than the higher $T_c$ phase. Meissner effect calculations from susceptibility measurements give values of 62% for sample A and 48% for sample B, both indicative of bulk superconductivity. The smaller Meissner effect of sample B may be a consequence of the smaller average particle size relative to the magnetic field penetration depth.

As seen in the SEM/EDX elemental maps of each sample (Figures 3c and 4c), the crystal morphologies of the two samples are distinctly different. Crystallites

(48) Kistenmacher, T. J. *Inorg. Chem.* **1987**, *26*, 3649.
(49) Eickenbusch, H.; Paulus, W.; Gocke, E.; March, J. F.; Koch, H.; Schollhorn, R. *Angew. Chem., Int. Ed. Engl.* **1987**, *26*, 1188.
(50) Bordet, P.; Chaillout, C.; Chenavas, J.; Hodeau, J. L.; Marezio, M.; Karpinski, J.; Kaldis, E. *Nature* **1988**, *334*, 596.

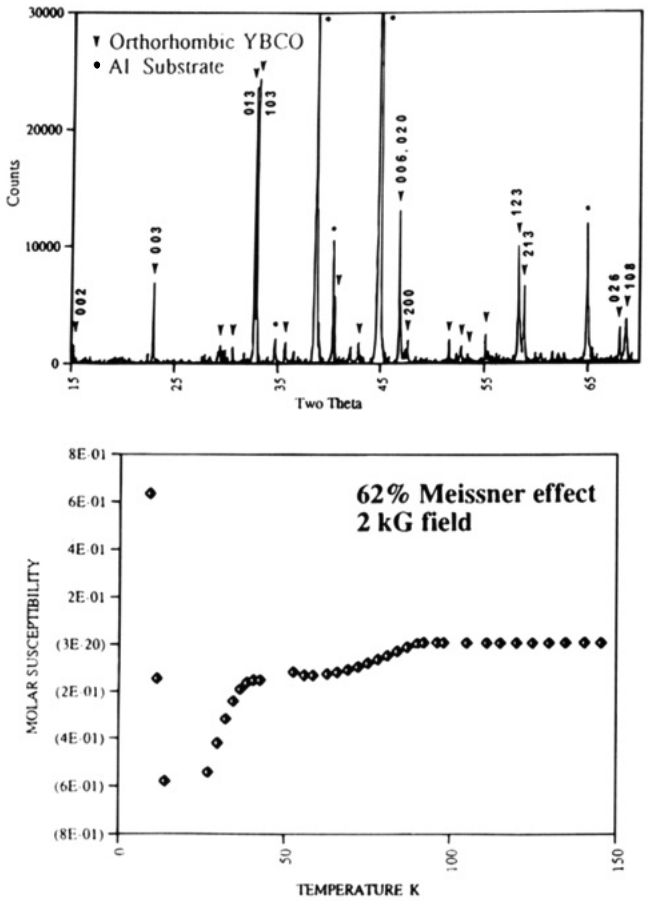


**Figure 3.** Solid-state synthetic product, fired at 950 °C for 24 h: (a, top) powder X-ray diffraction pattern; (b, middle) magnetic susceptibility; (c, bottom) EDX elemental maps. Bright areas indicate an abundance of the element, dark areas the absence of the element.

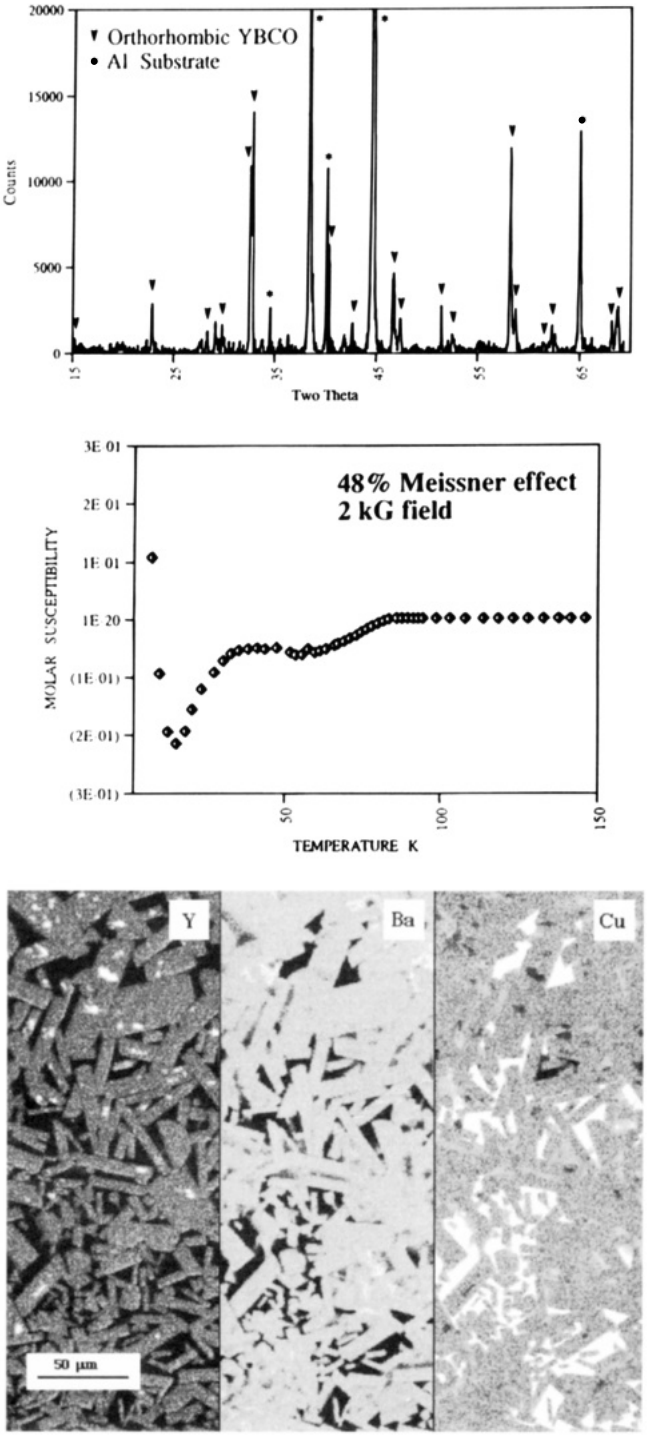


**Figure 4.** Sol−gel synthetic product, fired at 950 °C for 24 h: (a, top) powder X-ray diffraction pattern; (b, middle) magnetic susceptibility; (c, bottom) EDX elemental maps.

in sample A (from the solid-state synthesis) are relatively large and blocky, whereas crystallites in sample B are generally smaller and have two distinct shapes: blocky and rodlike. Since the particle size of the prefired materials was not determined, it is not known whether this difference in crystal size and morphology is a direct consequence of the prefired particle size or not. Interestingly, although different synthesis methods were used, both of these samples show the same type of inhomogeneity in the EDX lateral maps. In both cases, there is segregation of barium from copper with high concentrations of copper between crystallites. In addition, there are pockets of high yttrium concentration within crystallites in both samples.

For the conventional solid-state synthesis this separation of elements could be considered to be an effect of insufficient grinding and sintering. In the sol−gel synthesis this same segregation of elements could be due to the difference in gelation rates or the thermodynamically favorable formation of $BaCO_3$ during gelation. However, the fact that the separation phenomena seen in the elemental maps are similar for both synthesis methods suggests that the inhomogeneous prod-

ucts observed represent the thermodynamically stable mixture of phases at 950 °C.[5,14,36] Indeed, the presence of high copper concentration between crystallites has been attributed previously to the formation of a liquid phase at ~950 °C.[36] This interpretation is consistent with the firing temperatures and observations reported here.

Elemental analysis (Table 2) indicates that samples A and B have very similar yttrium, barium, copper, and carbon contents. However, both are slightly yttrium-poor and significantly copper-rich relative to the calculated values for $YBa_2Cu_3O_{6.8}$. The reasons for these deviations are not understood at present; the high copper content is particularly difficult to explain. Perhaps yttrium and barium are removed by reaction with the alumina crucible and by evaporation of volatile compounds, respectively. In any case, the fact that the analyses for samples A and B are very similar suggests that this nonstoichiometry is probably not a reflection of the stoichiometry of the reaction mixtures since the synthetic methods employed utilized completely different reactants.

Sample C was fired to 700 °C for 48 h and is representative of numerous sol–gel samples made during the course of this work. Pyrolysis at 700 °C generally gives products which appear to be a single tetragonal phase by X-ray diffraction. Attempts were made to convert the single phase tetragonal samples obtained at 700 °C to the orthorhombic phase by slow cooling in oxygen and/or annealing in oxygen for 5–12 h at temperatures ranging from 450 to 650 °C with no success. Since annealing does not readily convert the material to the orthorhombic phase, we believe this tetragonal phase is the oxycarbonate phase, $YBa_2Cu_3(CO_3)_xO_{7-\delta}$,[27–29] rather than the tetragonal $YBa_2Cu_3O_{7-\delta}$ phase. The lattice parameters for sample C correspond more closely to those of the oxycarbonate phase (Table 1), and elemental analysis (Table 2) indicates the carbon content of these materials is ~0.55 wt % (comparable to that of the oxycarbonate phase). IR spectra show a peak at 1400 $cm^{-1}$ (cf. 1403 and 1450 $cm^{-1}$ for the oxycarbonate phase).[28] We do not observe a peak at 1450 $cm^{-1}$ as reported by Gotor et al.,[28] but it is possible that the peak they observed in this region was from $BaCO_3$ or some other carbonate salt (for which the carbonate peak generally occurs in the region 1435–1441 $cm^{-1}$). In addition, iodometric titrations indicate an oxygen content corresponding to $YBa_2Cu_3O_{6.8}$, which is very similar to the oxygen content for the oxycarbonate phase ($YBa_2Cu_3(CO_3)_{0.2}O_{6.7}$) described by Karen and Kjekshus.[29]

The X-ray diffraction pattern and EDX elemental maps for sample C are shown in Figure 5. For this sample, as mentioned above, the X-ray diffraction pattern, IR spectrum, oxygen content, and carbon elemental analysis are consistent with the oxycarbonate phase. Accordingly, magnetic susceptibility measurements did not show the presence of any superconducting phases. The EDX elemental maps show irregular particles and some evidence of zoning. In general, elemental segregation occurs to a much smaller degree in sample C than in samples A and B. However, along the inner edge of the zoning, higher concentrations of yttrium can be seen in a few of the particles, and this may be an indication of how the yttrium pockets are

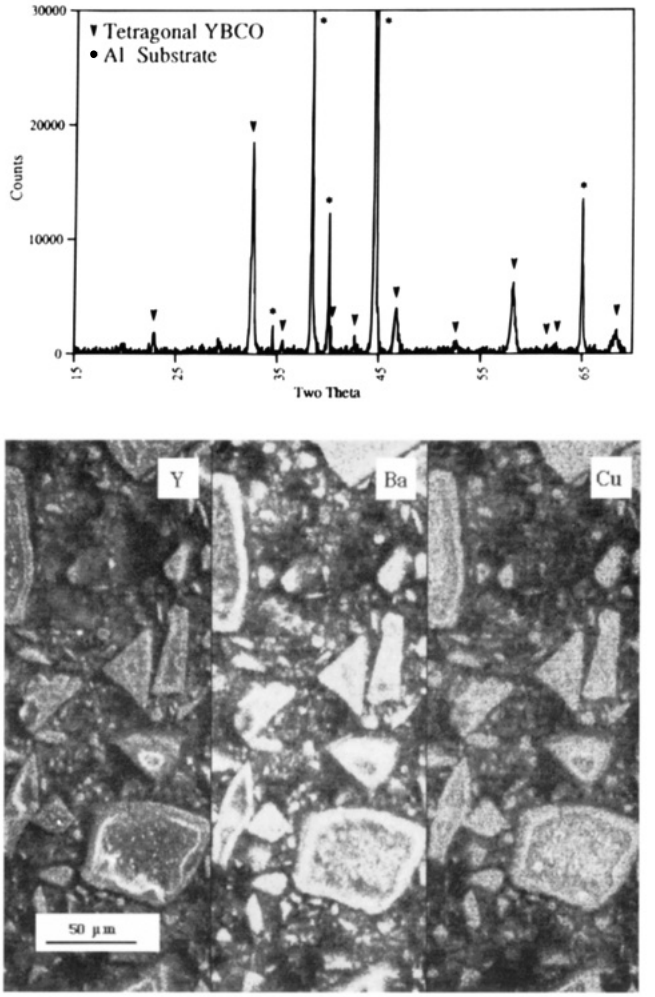


**Figure 5.** Sol–gel product fired at 700 °C for 48 h: (a, top) powder X-ray diffraction; (b, bottom) EDX elemental maps.

formed in samples A and B. A more detailed study would be needed to confirm this hypothesis. In natural mineral systems zoning occurs in solid solutions where the core phase represents the initial phase and the outer zone represents subsequent growth; zoning generally indicates that the total system was not at thermodynamic equilibrium under the reaction conditions. Such zoning could also be a consequence of incomplete reaction of an intermediate (e.g., tetragonal) phase. Therefore, the zoning seen in these maps was taken as an indication that the system had not been given sufficient time to reach equilibrium. To investigate this possibility, sample D was fired to 700 °C for 2 weeks.

The X-ray diffraction pattern from sample D (Figure 6a) shows the product of this extended firing to be mostly orthorhombic $YBa_2Cu_3O_{7-\delta}$. The splitting of the appropriate peaks is not as pronounced as it is for the fully oxygenated orthorhombic phase; this may be due to a slightly lower oxygen content, e.g., an oxygen content corresponding to $\delta \sim 0.3$. Magnetic susceptibility data (Figure 6b) indicates a single superconducting phase with a $T_c$ of 88 K. The Meissner effect is calculated to be 18%, which is not as high as that of samples A and B. The lower Meissner effect may be a consequence of incomplete conversion to the orthorhombic phase, or it may be a consequence of a smaller particle size to magnetic penetration depth ratio. Elemental maps of this product are shown in Figure 6c. The particles are irregular in shape, but zoning is less

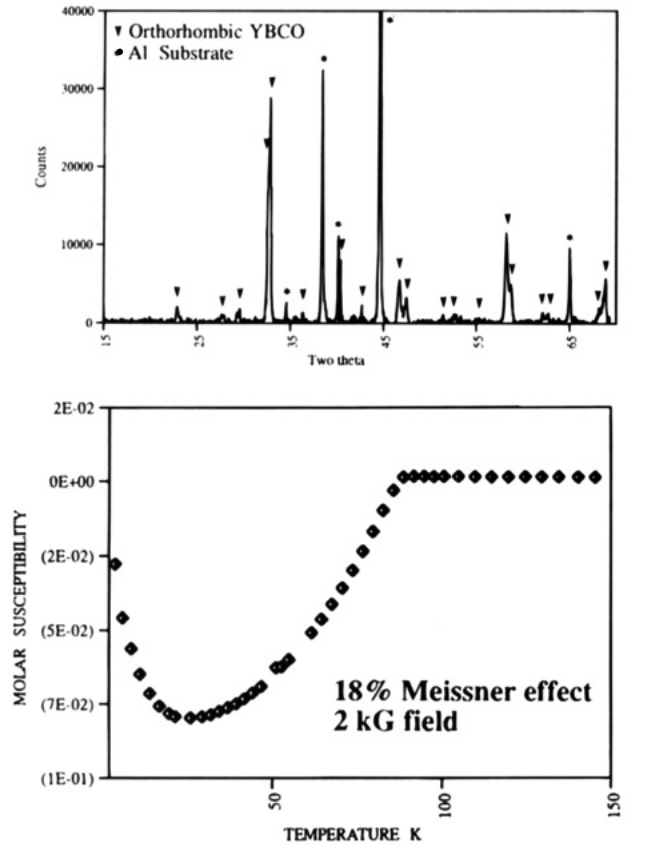


**Figure 6.** Sol–gel product fired at 700 °C for 2 weeks: (a, top) powder X-ray diffraction pattern; (b, middle) magnetic susceptibility; (c, bottom) EDX elemental maps.

evident than for sample C and the particles are generally homogeneous with no evident elemental separation. Most striking is the lack of high copper concentrations between crystallites which are observed in samples A and B. There are also no pockets of high yttrium concentration within crystallites.

On the basis of the apparent homogeneity as seen by EDX lateral mapping, the sharp single superconducting onset at 88 K, and the diffraction pattern, we conclude that the product of extended low-temperature (700 °C) firing contains higher quality orthorhombic $YBa_2Cu_3O_{7-\delta}$ than that produced by firing the gel or solid state reactants to 950 °C for 24 h. Further, because the inhomogeneities observed by EDX lateral elemental mapping appear to be greater for the gel sample fired to 950 °C than for gel fired to 700 °C even for relatively short firing times (e.g., sample C), it appears that a major source of elemental segregation may be due to impurity phase formation in the temperature range between 700 and 950 °C. Further studies are underway to determine if this is indeed the case.

## Conclusions

Although the 2-(2-methoxyethoxy)ethanol solvent system described here produces nearly ideal homogeneous stoichiometric starting solutions for the sol–gel synthesis of $YBa_2Cu_3O_{7-\delta}$, homogeneity in the alkoxide starting solution does not guarantee homogeneity in the final product. Gels fired to 950 °C for 24 h appear to be single-phase orthorhombic $YBa_2Cu_3O_{7-\delta}$ by X-ray diffraction, but magnetic susceptibility indicates the presence of at least two superconducting phases, similar to products of our solid-state synthesis. This last point highlights the importance of the use of characterization methods other than and in addition to X-ray diffraction. Our studies show that products which appear to be single phase by X-ray diffraction can be compositionally inhomogeneous on the micrometer scale and may in fact be multiphase in terms of physical properties such as superconductivity.

Gels fired to 700 °C for 24–48 h appear to be the oxycarbonate tetragonal phase by XRD, IR data, and elemental analysis. Elemental maps show solid solution-type zoning, indicating a nonequilibrium state. Gels fired to 700 °C for two weeks are essentially orthorhombic by XRD and have a single superconducting onset temperature at 88 K. Elemental maps of this material show a more homogeneous product than products of high-temperature firing. These studies indicate that kinetic effects are important at these relatively low firing temperatures, and that substantial micrometer-scale inhomogeneity may be introduced at temperatures between 700 and 950 °C. The finding that longer reaction times are necessary in order to obtain superconducting orthorhombic material at reduced firing temperatures, along with the complex phase equilibria and common carbonate contamination problem in this system, may explain why the sol–gel synthesis of $YBa_2Cu_3O_{7-\delta}$ has previously met with limited success. Finally, EDX compositional mapping is a powerful technique for evaluating homogeneity in synthetic solid-state products in general and is especially useful for assessing the homogeneity of sol–gel intermediates and products.

**Acknowledgment.** This work was supported by the National Science Foundation (DMR-9215308). Support for C.S.H. was provided by the Department of Education GAANN program. We thank the following people from the University of Oregon for their help: Eric Shabtach for the TEM micrographs; Mike Shaffer for help with the SEM/EDX mapping; and Dr. Thomas Novet for help with the Faraday balance.

CM940369L